

Sizing and technical study of a solar photovoltaic/thermal system: Application in Bejaia area

D. Rekioua^{1,*}, S. Belaid¹, T. Rekioua¹

¹Laboratoire de Technologie Industrielle et de l'information (LTI), Faculté de Technologie, Université de Bejaia, 06000 Bejaia, Algérie

ARTICLE INFO

Article Type:

Research Article

Article History:

Received: 24December2021

Revised: 11 February 2022

Accepted: 22 February 2022

Published: 30 March 2022

Editor of the Article:

M. E. Şahin

Keywords:

Photovoltaic

Solar thermal

Storage tank

Heater exchanger

ABSTRACT

In this paper, a hybrid renewable energy system is proposed, which consist of solar photovoltaic (PV), solar thermal, and battery energy storage. A photovoltaic pumping system and solar water heating have been combined to ensure that the water level in the tank is kept at a maximum value. It is obtained an entire system tacking account the benefits of the PV system and of a solar thermal system which allow us to obtain better performances of the global studied system. An application has been made on the Bejaia location in the northeast of Algeria which has a good solar irradiance, and a case study is conducted. To identify the system, measurements were carried out on different days. The evolution of temperatures during different profiles at various solar irradiance has been made by simulation under MATLAB/Simulink and compared to the experimental ones. The calculation of experimental effectiveness of heat exchanger has been made during two different days. It varies in our case from 0.5747 to 0.5815. So, solar irradiance does not influence it, but depends on the material nature, the exchange surface and the type of flow. Also, it is obtained a daily efficiency which varies from 30.75% to 35.58%. This efficiency decreases with solar irradiance increasing. The results obtained from simulation agree with experimental ones.

Cite this article: D. Rekioua, S. Belaid, T. Rekioua, "Sizing and technical study of a solar photovoltaic/thermal system: Application in Bejaia area," *Turkish Journal of Electromechanics & Energy*, 7(1), pp.3-14, 2022.

1. INTRODUCTION

The exploitation of solar energy by using solar collectors is composed of two distinct technologies: solar thermal energy, and photovoltaic energy [1]. Hot water is one of the most popular and efficient applications of solar thermal energy. Indeed, heating is an everyday problem for isolated areas. Through technological development, solar heater (SH) has greatly evolved technically, aesthetically, and thermally. It is generally made up of two collectors of square shape and a vertical cylindrical tank.

Different studies and reviews are devoted to solar HPV/T hybrid systems [2-5]. Some works are reviews on these systems that allow readers to better understand them. In [2], authors give a wide range of details on advanced type collectors, working fluids, analyzing methods to evaluate performance, thermodynamic approaches, optimization of design parameters and design parameters and mass flow rates, techniques to improve performance, and comparative studies. They conclude that these systems may be one of the main clean energy technologies in the future. Also in [3-5], a review of PV-Thermal collectors is detailed. Other studies are based on an economical study on hybrid photovoltaic/thermal (HPV/T) systems with battery storage. In [6], the study allows designing the different

components (photovoltaic panels, solar thermal modules, and the storage battery), to obtain the lowest cost. In the study [7], two configurations of the PV/T system were presented to compare the evaluation of electrical and thermal performances. The study was based only on analytical and simulation under MATLAB.

This work aims to study a solar photovoltaic/thermal system. The solar thermal system is a monobloc thermo-siphon, which consists of two flat plate temperature collectors and a horizontal storage tank with a heat exchanger. The photovoltaic system is equipped with a moto-pump [8-10]. The purpose of the proposed system is to obtain energy by PV pumping system which supplied the water tank of the solar thermal system. A photovoltaic pumping system and solar water heating have been combined to ensure that the water level in the tank is kept at a maximum value.

It is obtained an entire system tacking account the benefits of the PV system and solar thermal system which allow us to obtain better performances of the global studied system. The obtained results show the role of this combination to use only solar energy.

Different studies on this idea were done in literature [11-15]. The evolution of temperatures during different profiles at various solar irradiance has been made by simulation under MATLAB/Simulink and compared to the experimental ones.

*Corresponding author e-mail: djamila.ziani@univ-bejaia.dz

The calculation of the experimental effectiveness of the heat exchanger and the daily efficiency has been made to show the influence of solar irradiance. For the hybrid system, an experimental test bench is installed in the laboratory. It is equipped with measurements instruments to measure the required data. In our case, we were interested to follow the evolution of the temperatures after each pump-down. Obtained results are presented and analyzed. To properly situate this work, the contribution made through this paper is focused on the following points:

- Photovoltaic pumping system and solar water heating have been combined to ensure that the water level in the tank is at a maximum value. It is obtained an entire system tacking account the benefits of PV and solar thermal system obtaining better performances of the global studied system.
- A detailed physical model of the hybrid system is established under MATLAB/Simulink environment, which consists of the PV system, the solar thermal system, and batteries. Experimental results are presented to confirm the obtained simulation results.

To accomplish the mentioned points above, this article is organized into five sections: Section 1 presents an introduction that gives an overall idea of the studied area. In section two, a description of the solar photovoltaic/thermal system is given. In section three, the study sizing of the studied system is explicitly detailed. Modeling and simulation of the global system are presented in section four. A hybrid solar photovoltaic/thermal system is proposed in section five with the different experimental and simulation results. Finally, the main conclusion of this work is presented.

2. DESCRIPTION OF SOLAR PHOTOVOLTAIC/THERMAL SYSTEM

Photovoltaic pumping system and solar water heating have been combined as in Figure 1 to ensure that the tank water level is kept at its maximum value.

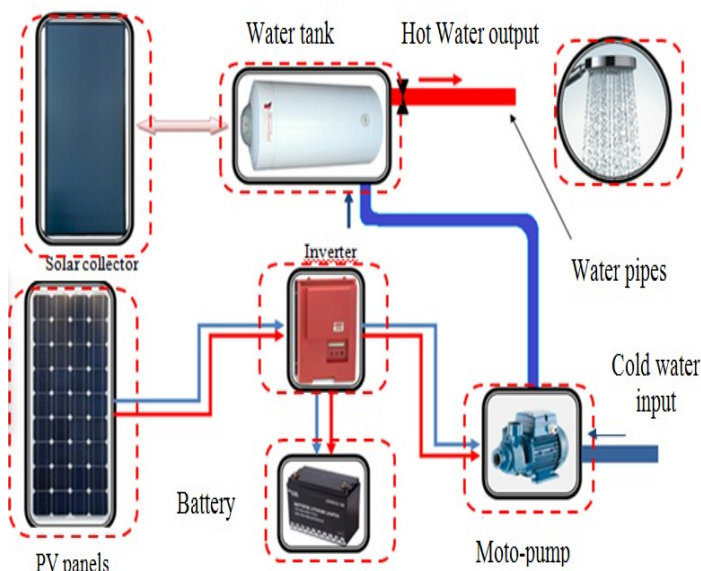


Fig. 1. The global system of solar PV/thermal system.

2.1. Solar Water Heater

In our case the solar water heater is designed mono bloc thermosiphon type, it consists mainly of two solar thermal collectors, connected in parallel, with a total sensing surface area is 4 m², a storage tank with a capacity of 400 liters, a thermally insulated pipelines, a security group, and an electric backup is integrated into the tank to ensure continuity of hot water production. The thermal system is represented in Figure 2. The characteristics of the solar water heater studied are summarized in Table 1.



Fig. 2. Thermosiphon solar water heater.

Table 1. Characteristics of thermosiphon solar water heater.

Parameters	Characteristics
Plan collector dimensions	1000 x 2000 x 100 mm
Nature of the absorbent surface and characteristic	Matte paint, Absorption $\alpha = 95\%$, Emission $E = 7\%$
Glazing	Transmissivity 83%, Thickness = 4 mm
Background of the map sensor	galvanized aluminum sheet
Connection line between the tank outlet and the inlet sensor	Length $L = 1000$ mm
The size of the storage tank	Length: $L = 1.20$ m, Capacity: 400 L, Output diameter of the tank = 0.33 m
Tubes(Nature and size)	Copper Tube Diameter $D = 10$ mm Length: $L = 1800$ mm

2.2. Photovoltaic Panels

The used photovoltaic panels shown in Figure 3 have the following characteristics in Table 2.



Fig.3. Photovoltaic panels of 80 Wp.

Table 2. PV parameters of SUNTECH STPO80S-12/Bb [16].

Symbol	Quantity	Value
P_{PV}	Photovoltaic power	80 Wp
I_{mpp}	Maximum current at MPP	4.58 A
V_{mpp}	The maximum voltage at MPP	17.5 V
I_{sc}	Short circuit current	4.95 A
V_{oc}	Open circuit voltage	21.9 V
α_{sc}	Temperature coefficient of short-current	3.00 mA/°C
β_{oc}	Voltage temperature coefficient	-150.00 V/°C

3. DESIGNED SYSTEM AND BEJAIA LOCATION

The study sizing has provided the different components of the studied system. The design of hot water is based essentially on the knowledge demand of the consumers.

3.1. Geographical Bejaia Location:

The application is made in Bejaia location in Algeria (Latitude 36°45.3522'N, Longitude 5°5.0598' E), which is located in the northeast region of Algeria in Figure 4. The solar irradiance and the temperature measured using the software Homer pro are given in Figure 5.

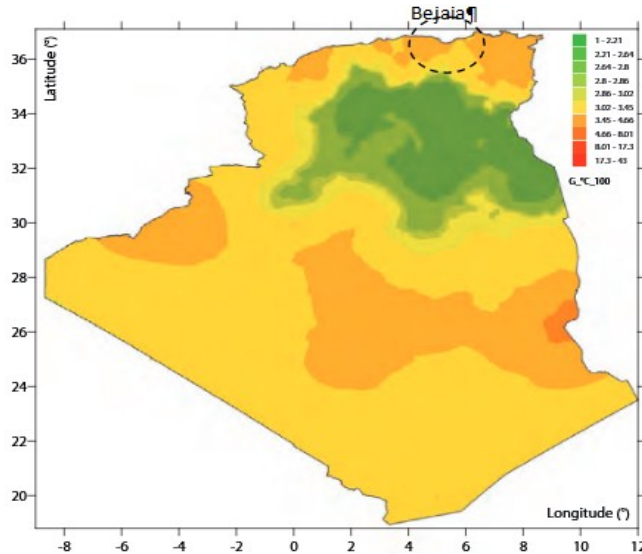


Fig. 4. The geographical position of the Bejaia area.

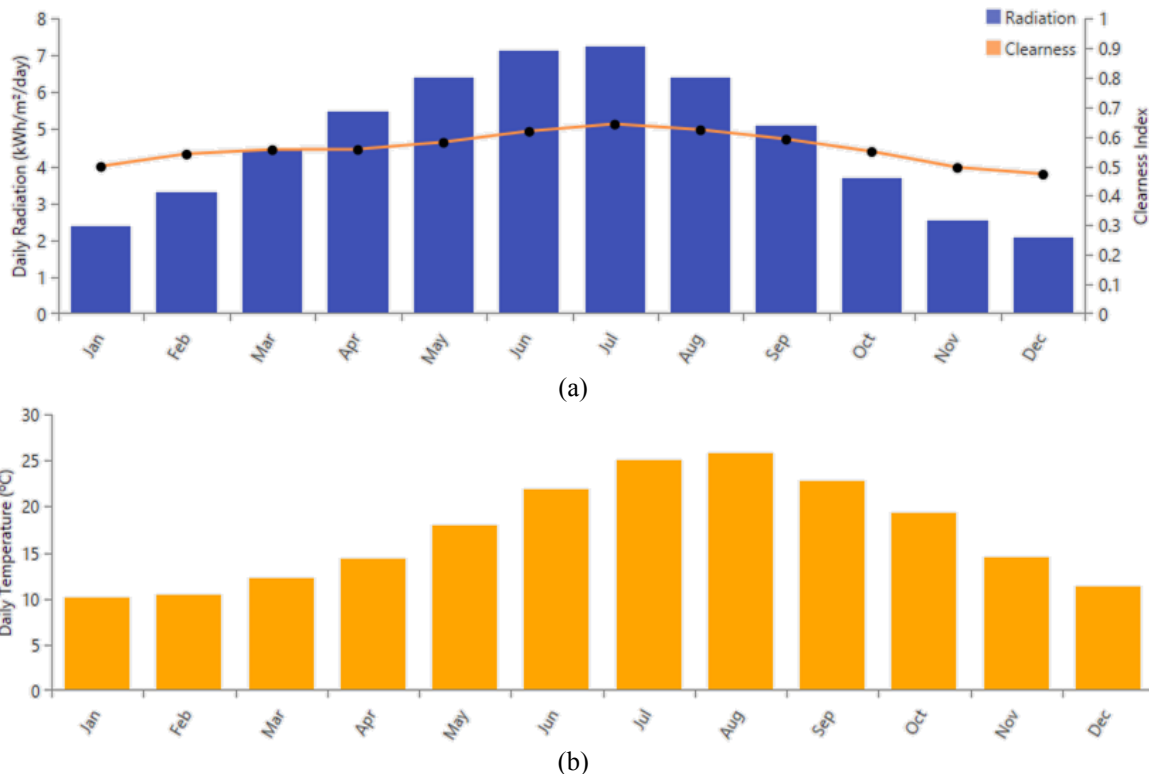


Fig. 5. Weather conditions at Bejaia area using Homer Pro Software; (a) Solar irradiance, (b) Ambient temperature during a year.

3.2. Sizing of Photovoltaic Panels

The design of the PV system is based on the exact knowledge of the load and solar radiation. The PV number is [17-18]:

$$N_{pv\text{-}serial} = \frac{E_{energy}}{E_{worst} \cdot \eta_{batt} \cdot \eta_{reg} \cdot \eta_{Lines}} \quad (1)$$

η_{batt} is the battery efficiency, η_{reg} is the electrical efficiency, E_{energy} is the load energy, E_{worst} is the worst value of solar irradiance;

The maximum voltage is estimated by [11]:

$$V_{pv\text{-}max} = 1.15 N_{pv\text{-}serial} \cdot U_{oc} \quad (2)$$

The parallel PV can be calculated as:

$$N_{pv\text{-}para} = \frac{U_{pv\text{-}max}}{V_{DC\text{-}bus}} \quad (3)$$

where $V_{DC\text{-}bus}$ is DC bus voltage, $U_{pv\text{-}max}$ is the maximal PV voltage value, $N_{pv\text{-}serial}$ is the serial number of PV panels.

Then, the panels' number is deduced:

$$N_{pv} = N_{pv\text{-}para} \cdot N_{pv\text{-}serial} \quad (4)$$

where: N_{pv} is the PV panels number, $N_{pv\text{-}para}$ is the parallel PV panels number and $N_{pv\text{-}serial}$ is the serial PV panels number.

The photovoltaic power will be:

$$P_{pv\text{-}totale} = N_{pv} \cdot P_{pv} \quad (5)$$

3.3. Sizing of Solar Sensors

The solar heater studied is a thermosiphon that consists of two parts. These are the flat plate collector and the storage tank. The first one has the role to capture the solar energy and to convert it into thermal energy via a plan collector designed for this purpose. The second part is to ensure the storage of this energy in a tank located above the flat plate collector to ensure the circulation of water. A thermally insulated circuit connects these two parts. In the laboratory, we have a system with two solar collectors with a storage tank with a capacity of 400 liters.

4. MODELING AND SIMULATION OF GLOBAL SYSTEM

4.1. Modeling of Solar Water Heaters

In this part, modeling of solar collector and the storage tank with Heat Exchanger is made. Then a simulation allows us to obtain the evolution of the temperatures T_c , T_b , and T_s .

4.1.1. Solar Collector Modeling

Consider the plane solar collector shown in Figure 6. Under steady-state conditions, the heat absorbed by the heat transfer fluid as it flows through the collector is equal to the heat gain from the collector subtracting heat losses.

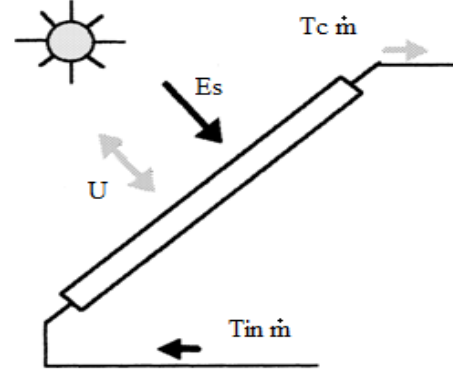


Fig. 6. Thermal balance of a solar collector plane.

$$\frac{\text{Accumulation of total energy}}{\text{Time}} = \frac{\text{Input of total energy}}{\text{Time}} = \frac{\text{Output of total energy}}{\text{-time}} \quad (6)$$

The absorbed energy of a solar flat plate collector can be calculated as follows:

$$Q_s = E_s \cdot A_c \cdot \tau \cdot \alpha \quad (7)$$

with: τ is the transmittance of the cover of the collector and α is the absorbance of the plate of the manifold.

The heat loss of the collector is given by [19]:

$$Q_l = U \cdot A_c \cdot (T_{abs} - T_a) \quad (8)$$

where: T_{abs} is the surface temperature of the absorber plate, T_a is the ambient temperature.

The heat loss of the collector can be calculated as follows:

$$Q_f = m \cdot c \cdot (T_c - T_{in}) \quad (9)$$

with: c is the specific heat capacity of the fluid, m the fluid mass

For simplicity, it is assumed that the fluid in the solar collector is completely mixed. Then the energy balance of the collector based on Equations (7), (8), and (9) can be given by:

$$\frac{d(\rho \cdot c \cdot V \cdot T_c)}{dt} = E_s \cdot A_c \cdot \tau \cdot \alpha - U \cdot A_c \cdot (T_{av} - T_a) + F_c \cdot \rho_{in} \cdot c_{in} \cdot T_{in} - F_c \cdot \rho_{out} \cdot c_{out} \cdot T_c \quad (10)$$

where: ρ is the fluid density, V is the volume of the fluid in the manifold, F_c is the volumetric flow rate, ρ_{in} and ρ_{out} are respectively the density of fluid at the input and c_{in} and c_{out} are respectively the specific heat capacity of the fluid at the input and the output of the collector.

The following assumptions are taken:

V : est constant and $\dot{m} = F_c \cdot \rho$

with:

$$\begin{cases} \rho_{in} = \rho_{out} = \rho \\ c_{in} = c_{out} = c \end{cases}$$

Taking into account the above assumptions, Equation (10) can be rewritten as follows:

$$\rho.c.V.\frac{dT_c}{dt} = E_s.A_c.\tau.\alpha - U_L.A_c(T_{av} - T_a) + m.c(T_{in} - T_c) \quad (11)$$

Due to the difficulty of measurement of T_{abs} , it is usual to express it in terms of temperature T_{av} , which represents the average of temperatures T_{in} , and T_c :

$$T_{ave} = \frac{T_c + T_{in}}{2} \quad (12)$$

Taking into account the correction factor F' which is called heat transfer or heat removal factor, it is obtained:

$$\rho.c.V.\frac{dT_c}{dt} = E_s.A_c.F'\tau\alpha - UF'.A_c(T_{av} - T_a) + m.c(T_{in} - T_c) \quad (13)$$

The optical efficiency is:

$$\eta_0 = F'.\tau.\alpha \quad (14)$$

And the overall heat loss coefficient is:

$$U_L = U.F' \quad (15)$$

By replacing expressions (14) and (15) in Equation (13), it is obtained:

$$\rho.c.V.\frac{dT_c}{dt} = E_s.A_c.\eta_0 - U_L.A_c(T_{av} - T_a) + m.c(T_{in} - T_c) \quad (16)$$

$$C = \rho cV \quad (17)$$

with: C is the overall heat capacity of the fluid

Finally, Equation (16) can be written as:

$$\frac{dT_c}{dt} = E_s.\frac{A_c.\eta_0}{C} - \frac{U_L.A}{C}(T_{av} - T_a) + \frac{m.c}{C}(T_{in} - T_c) \quad (18)$$

4.1.2. Modeling of the Storage Tank with Heat Exchanger

In the following case, the model is built up as a hot water storage tank that contains a heat exchanger coil in Figure 7.

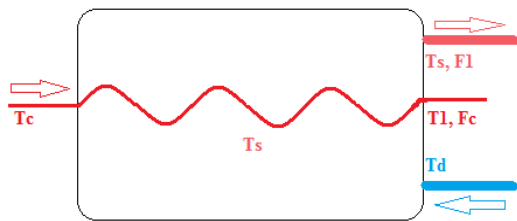


Fig. 7. Hot water tank with heat exchanger.

It is assumed that the storage tank is completely mixed and the supplied water temperature T_d is constant. In this case, the energy balance equations for the storage tank can be written as [20]:

$$\frac{d[\rho.c.V_{st}.T_c]}{dt} = F_l.\rho_l.c_{pl}.(T_d - T_s) + F_c.\rho_c.c_{p2}.(T_c - T_l) \quad (19)$$

where T_c is the temperature of the solar liquid which comes from the collector, T_l is the solar liquid temperature which returns to the collector, T_s is the extracted water temperature, F_l is the volumetric flow rate of the load, F_c is the collector volumetric flow rate and V_{st} is the storage tank volume.

Another equation is needed to find T_l is used:

$$F_c.\rho_c.c_{p2}.(T_c - T_l) = U_c.A_e \frac{\Delta T_c - \Delta T_l}{\ln\left(\frac{\Delta T_c}{\Delta T_l}\right)} \quad (20)$$

$$\Delta T_c = T_c - T_s \quad (21)$$

$$\Delta T_l = T_l - T_s$$

where A_e is the surface of the coil.

The equation assumes that there are no changes in the coil heat storage coil, so it can be assumed that the coil is in a steady state. In this case, Equations (19) and (20) will be written as below:

$$\rho.c.V_{st}.\frac{dT_s}{dt} = F_l.\rho.c.(T_d - T_s) + F_c.\rho.c.(T_c - T_l) \quad (22)$$

$$F_c.\rho.c.(T_c - T_l) = U_c.A \frac{\Delta T_c - \Delta T_l}{\ln\left(\frac{\Delta T_c}{\Delta T_l}\right)} \quad (23)$$

Using Equation (23), the temperature T_l is given as a function of T_s and the output values T_c and F_c .

$$T_l = (T_c - T_s)e^{-(U_c.A/c.F_c.\rho)} + T_s \quad (24)$$

The evolution of the temperatures T_c , T_l , and T_s using the different equations and simulated under MATLAB/Simulink as in Figure 8.

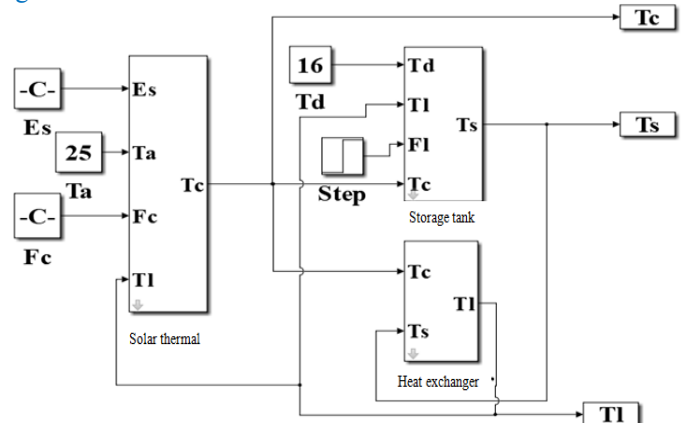


Fig. 8. Block diagram of the solar water heater under MATLAB/Simulink.

4.2. Simulation Results Under Constant Conditions

The obtained simulation results are represented in Figure 9.

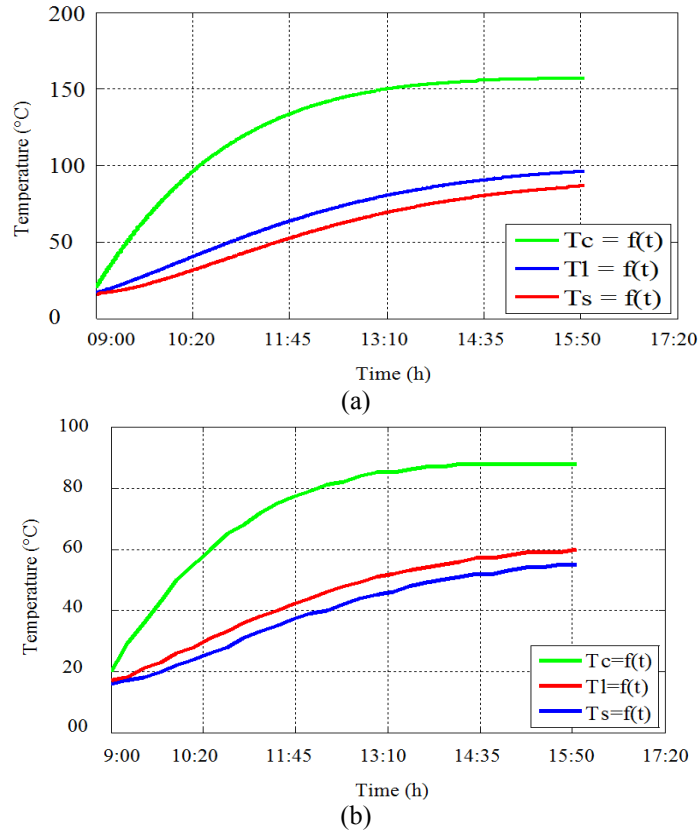


Fig. 9. Evolution of the different temperatures under two different tests; (a) Test1 ($E_s=1000 \text{ W/m}^2$, $T_a= 25 \text{ }^\circ\text{C}$), (b) Test 2 ($E_s=750 \text{ W/m}^2$, $T_a= 28 \text{ }^\circ\text{C}$).

The different temperatures follow a similar evolution for both conditions. The collector output temperature T_c reaches $152 \text{ }^\circ\text{C}$ in the first profile and $85 \text{ }^\circ\text{C}$ in the second profile.

4.2 Simulation Results Under Variable Conditions

Then, it has been chosen two different profile days with variable conditions of solar irradiance and temperature. For the first profile and the second one, it is obtained respectively the different results in Figures (10) and (11).

The obtained results are compared and analyzed. It can be seen that temperatures follow a similar evolution for both different conditions. They increase in the morning around 9 am and reach a maximum around 2 pm. The collector output temperature T_c reaches $70 \text{ }^\circ\text{C}$ the first day and $80 \text{ }^\circ\text{C}$ the second day. Also, the input temperature of the collector T_{in} reaches $55 \text{ }^\circ\text{C}$ on the first day and $65 \text{ }^\circ\text{C}$ on the second day. The storage temperature T_s starts to increase after the thermosiphon is initiated, reaching $45 \text{ }^\circ\text{C}$ on the first day and $55 \text{ }^\circ\text{C}$ on the second day.

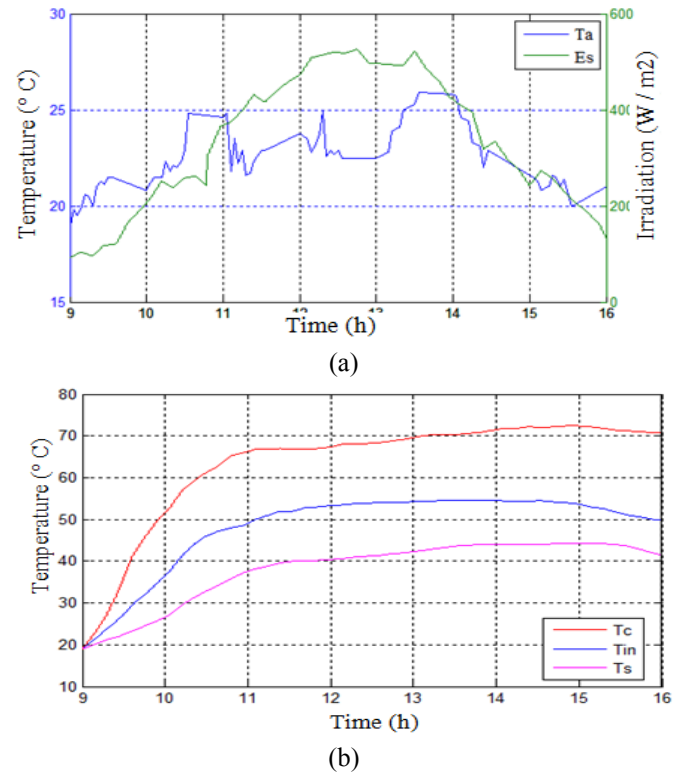


Fig.10. Evolution of temperatures during the first profile; (a) First profile, (b) Temperature variations.

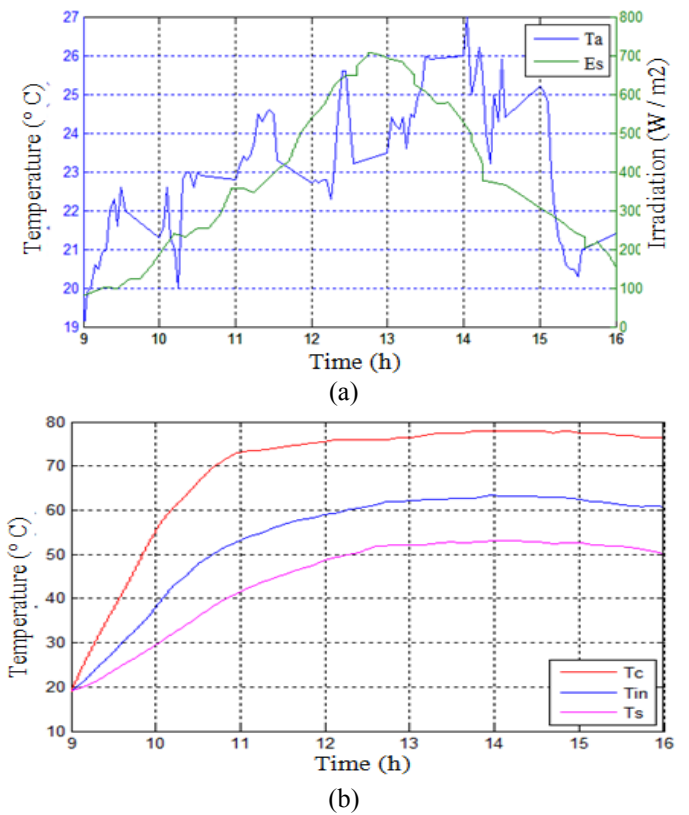


Fig.11. Evolution of temperature during the second profile; (a) Second profile, (b) Temperatures variations.

4.3. Modeling and Simulation of PV System

Electrical characteristic is obtained using the following equations [21-22]:

$$I_{pv} = I_{ph} - I_d - I_{Rsh} \quad (25)$$

$$I_{pv} = I_{ph} - I_0 \left[\exp\left(\frac{q \cdot (V_{pv} + I_{pv} \cdot R_s)}{A n_s k T_j}\right) - 1 \right] - \frac{V_{pv} + R_s \cdot I_{pv}}{R_{sh}} \quad (26)$$

The photocurrent, I_{ph} , is directly dependent upon both solar irradiation and panel temperature. It may be written in the following form [1]:

$$I_{ph} = P_1 \cdot E_s \cdot \left[1 + P_2 \cdot (E_s - E_{s-STC}) + P_3 \cdot (T_j - T_{j-STC}) \right] \quad (27)$$

Where: E_s solar irradiation in the panel plane (W/m^2); E_{s-STC} solar irradiation at STC conditions ($1000 W/m^2$), and T_{j-STC} to the STC panel temperature ($25^\circ C$), P_1 , P_2 , and P_3 are constant parameters.

The polarization current I_d of junction PN, is given by the expression [1], [23]:

$$I_d = I_0 \cdot \left[\exp\left(\frac{q \cdot (V_{pv} + R_s \cdot I_{pv})}{A n_s \cdot k \cdot T_j}\right) - 1 \right] \quad (28)$$

$$I_0 = P_4 \cdot T_j^3 \cdot \exp\left(-\frac{E_g}{K \cdot T_j}\right) \quad (29)$$

With: I_0 saturation current (A), q the elementary charge (eV), k Boltzmann's constant, A ideality factor of the junction, T_j : junction temperature of the panels ($^\circ K$) and R_s , R_{sh} (Ω) resistors of series and shunt.

$$I_{sh} = \frac{(V_{pv} + R_s \cdot I_{pv})}{R_{sh}} \quad (30)$$

$$I_{pv} = P_1 \cdot E_s \cdot \left[\frac{1 + P_2 \cdot (E_s - E_{s-STC})}{1 + P_3 \cdot (T_j - T_{STC})} \right] - P_4 \cdot T_j^3 \cdot \exp\left(-\frac{E_g}{K \cdot T_j}\right) \cdot \left[\exp\left(\frac{q \cdot (V_{pv} + R_s \cdot I_{pv})}{A \cdot n_s \cdot K \cdot T_j}\right) - 1 \right] - \frac{(V_{pv} + R_s \cdot I_{pv})}{R_{sh}} \quad (31)$$

Equation (32) can be solved using the function 'fsolve' contained in toolboxes of MATLAB which is based on the least-squares method in Figure 12. With a numerical resolution and the use of PV data sheets, we establish the seven constant parameters P_1 , P_2 , P_3 , P_4 , the coefficient A , and the resistance R_s and R_{sh} of the PV model. Module manufacturers frequently include short-circuiting current I_{sc} , open-circuit voltage V_{oc} , and the point of optimum power (I_{mpp} , V_{mpp}). Three extra equations are necessary to obtain all seven parameters. The parameter P_2 must be calculated using sites with varied solar irradiance values. Points with various temperatures are also required for the parameter P_3 . A convergence test is made on the function $F(X, X_0)$, where X_0 and

X are respectively the initial conditions and the calculated seven parameters [1].

$$\begin{cases} I(V_{oc}) = 0 \\ I(0) = I_{sc} \\ I(V_{mpp}) = I_{mpp} \\ \left. \frac{dP}{dV} \right|_{P=P_{mpp}} = I_{mpp} + \left. \frac{dI}{dV} \right|_{V=V_{mpp}}^{I=I_{mpp}} = 0 \end{cases} \quad (32)$$

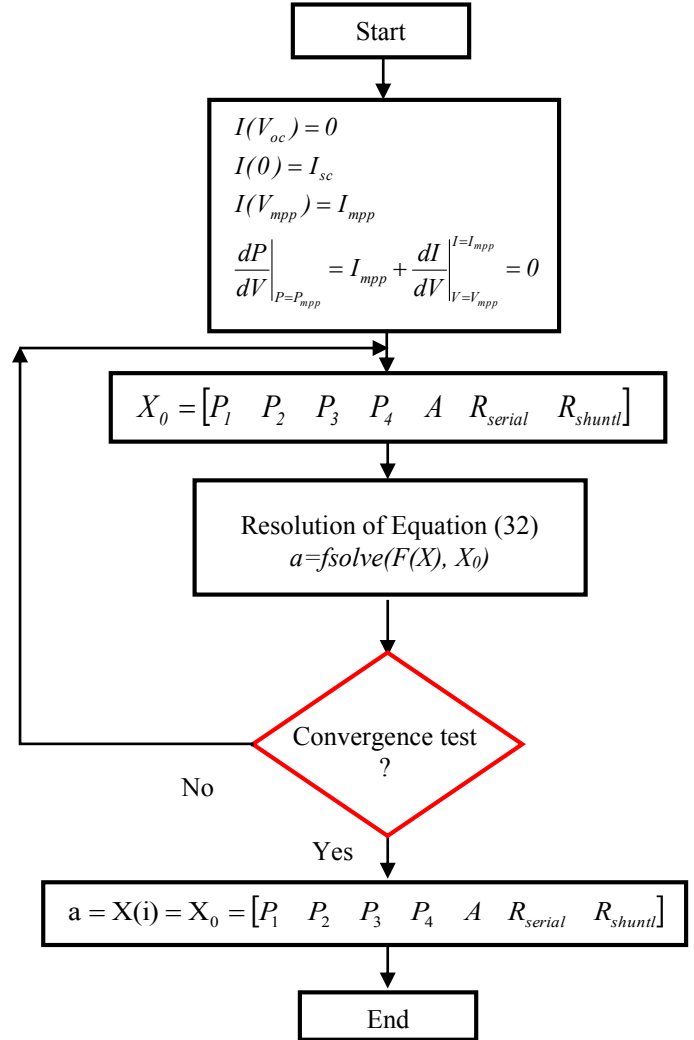


Fig. 12. Flowchart for resolution of the seven parameters.

The used PV test bench is represented in Figure 13. The used panel is a solar SUNTECH STPO80S-12/Bb of 80Wp. To measure electrical characteristics, a test bench is realized. The PV system must insert a variable load that allows it to absorb the power of the photovoltaic panel. The experimental electrical characteristics were compared to those obtained by simulation in Figure 14.

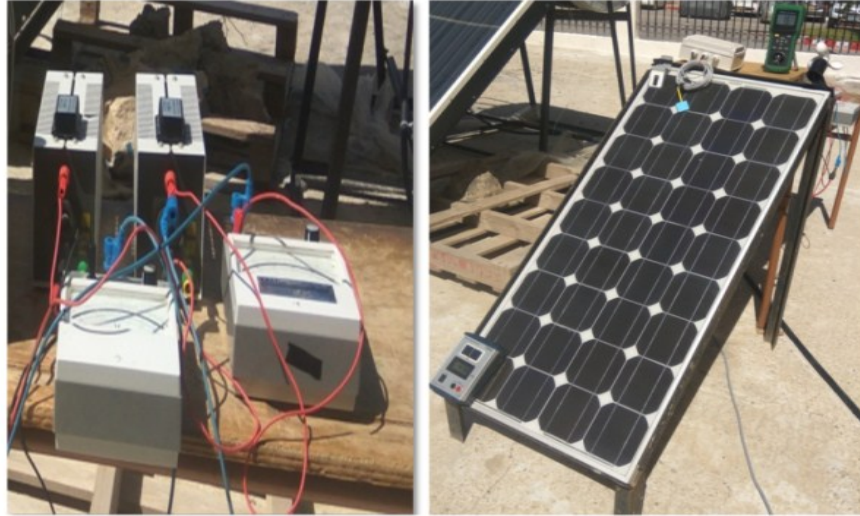


Fig. 13. Photovoltaic experimental test bench.

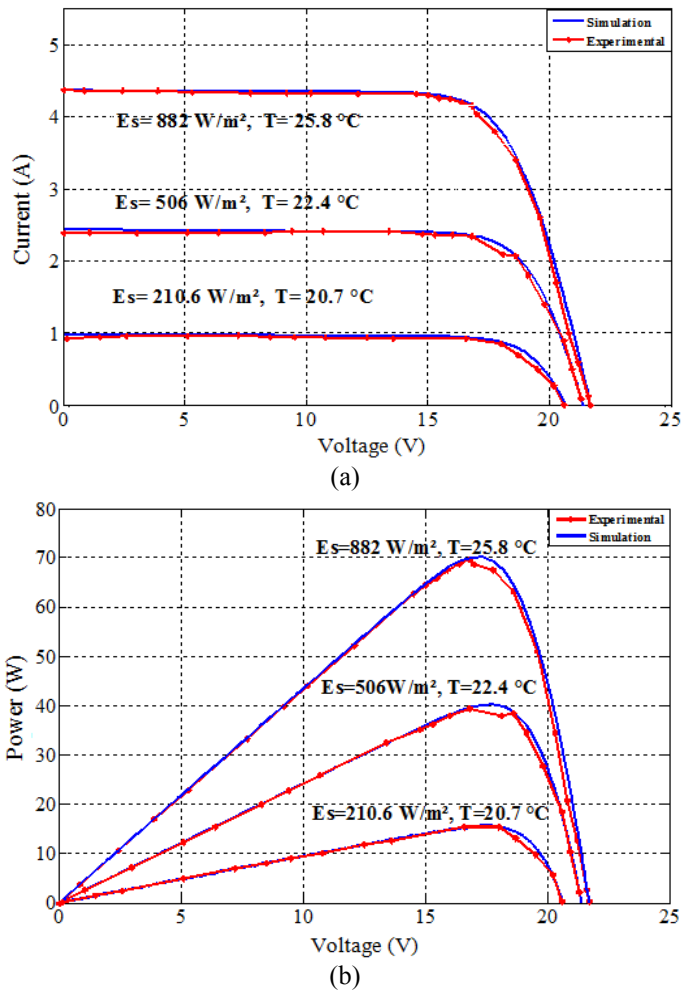


Fig. 14. Photovoltaic electrical characteristics. (a) $I_{pv}(V_{pv})$, (b) $P_{pv}(I_{pv})$.

5. EXPERIMENTAL HYBRID SOLAR PHOTOVOLTAIC/THERMAL SYSTEM

The experimental equipment is located in the Laboratory of the University of Bejaia. It is a coastal city in the North East of Algeria. In our work, a photovoltaic pumping system and solar water heating have been combined to ensure that the water level in the tank is kept at a maximum value. It is obtained an entire system taking into account the benefits of the PV system and solar thermal system which allow us to obtain better performances of the global studied system. The solar thermal prototype used for the experimental study is equipped with measurement instruments to measure the required data.

5.1 Experimental Effectiveness Heat Exchanger Calculation

Different tests were conducted on two different days. Figures (15) and (16) show the evolution of measured temperatures respectively during the first and the second profile day. For the first day, a calculation of the different temperatures average gives $T_{in}=54.14 \text{ }^\circ\text{C}$, $T_c=69.91 \text{ }^\circ\text{C}$, and $T_s=42.8 \text{ }^\circ\text{C}$. The effectiveness heat exchanger is calculated as follows [24]:

$$\varepsilon = \frac{T_c - T_{in}}{T_c - T_s} \quad (33)$$

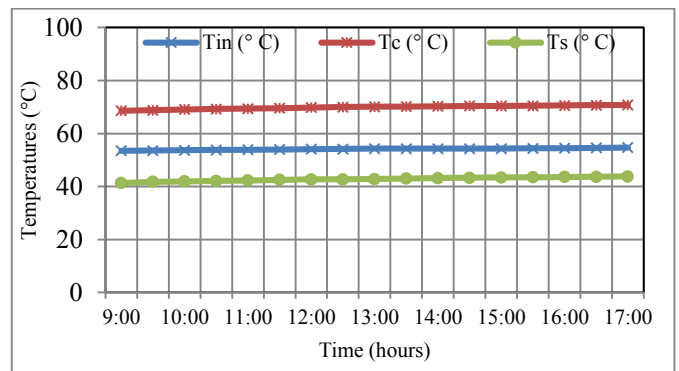


Fig. 15. Evolution of measured temperatures T_{in} , T_c , and T_s during the first profile day.

This gives for the first profile day efficiency of: $\epsilon_1=0.5815$. This value is relatively good, but it can be improved either by increasing the surface of the exchanger or by adding a propeller agitator inside the tank.

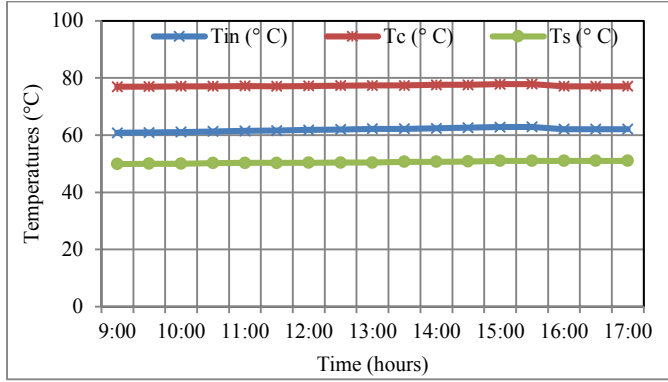


Fig. 16. Evolution of measured temperatures T_{in} , T_c , and T_s during the second day.

A calculation of the different temperatures average for the second profile day is obtained: $T_{in}=61.90$ °C, $T_c=77.29$ °C, and $T_s=50.53$ °C. This gives for the second profile day efficiency of $\epsilon_2=0.5747$. It is noticed that the efficiency of the exchanger is nearly the same for both profiles. So the variation of the solar irradiation does not influence the efficiency, which depends on the material nature, the exchange surface, and the type of flow.

5.2. Experimental Daily Efficiency Calculation

The daily efficiency is defined as the ratio between the energy of the storage (output), and the energy received (input) by the system. It can be written as [25-26]:

$$\eta_{daily} = \frac{\sum Q_{energy} - \sum Q_{losses}}{\sum A_c \cdot E_s} \quad (34)$$

with: Q_{energy} is the recovered energy, Q_{losses} are global losses from the tank.

The useful energy recovered by the collector over the day is given by [27]:

$$\sum Q_{energy} = A_c \cdot \eta_0 \cdot \sum E_s - A_c \cdot U_L \cdot \sum (T_s - T_a) \quad (35)$$

The energy lost by the storage tank over the day is given by

$$\sum Q_{losses} = U_{cu} \cdot A_{cu} \cdot \sum (T_s - T_a) \quad (36)$$

with: U_{cu} the coefficient of overall losses of the tank, in our case, is estimated at 2.10 W/m².°C [2].

The parameters varying with time in the equations are the ambient temperatures, the temperatures of the absorber, storage temperatures, and solar irradiance. It is chosen a cloudy and a sunny profile day to calculate the daily efficiency in Figure 17.

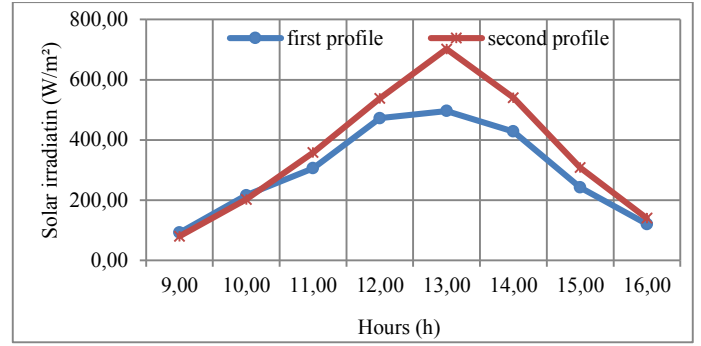


Fig. 17. Two different profile day solar irradiation.

After measuring the different temperatures during a first profile day, it is obtained in Table 3.

Table 3. Calculations of $(T_s - T_a)$ during a first profile day.

Hours	E_s (W/m ²)	T_a (°C)	T_s (°C)	$T_s - T_a$ (°C)
9:00	92,00	19,00	19,50	0,50
10:00	216,00	20,80	27,00	6,20
11:00	306,00	24,60	37,90	13,30
12:00	472,00	23,80	40,10	16,30
13:00	496,00	22,50	42,70	20,20
14:00	428,00	25,80	44,00	18,20
15:00	242,00	21,60	46,20	24,60
16:00	120,00	21,00	43,30	22,30
$\sum E_s = 2372,00$				$\sum (T_s - T_a) = 121,60$

Using Equations (35) and (36), it is found:

$$\sum Q_{energy} = 4185.58 \text{ W}, \sum Q_{losses} = 809.68 \text{ W}, \sum A_c \cdot E_s = 9448 \text{ W}$$

And finally, the daily efficiency (Equation (34)) is found. For the second profile day, it is obtained as in Table 4.

Table 4. Calculations of $(T_s - T_a)$ during a second profile day.

Hours	E_s (W / m ²)	T_a (°C)	T_s (°C)	$T_s - T_a$ (°C)
9:00	80,00	19,00	19,00	0,00
10:00	202,00	21,30	30,00	8,70
11:00	358,00	22,80	41,60	18,80
12:00	538,00	22,70	48,70	26,00
13:00	702,00	23,50	50,30	26,80
14:00	540,00	26,00	52,60	26,60
15:00	308,00	25,20	52,70	27,50
16:00	140,00	21,40	50,00	28,60
$\sum E_s = 2868,00$				$\sum (T_s - T_a) = 163,00$

Using Equations (35) and (36), it is found:

$$\sum Q_{energy} = 4613.6 \text{ W}, \sum Q_{losses} = 1085.35 \text{ W}, \sum A_c E_s = 11472 \text{ W}$$

And finally, the daily efficiency (Equation (34)) is found. It is noticed that the daily efficiency decreases with solar irradiance increasing.

5.3 Comparison of Simulation and Experimental Results

In Figure 18, the simulation results and practical ones for respectively the first and second tests are superimposed. It can be seen that the simulation and experimental results are in good concordance.

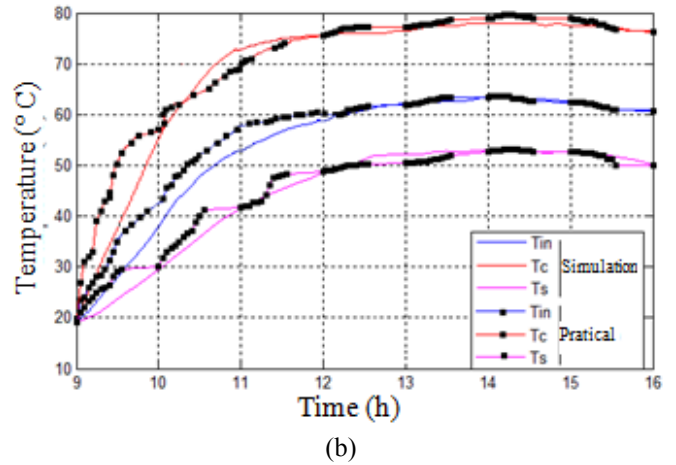
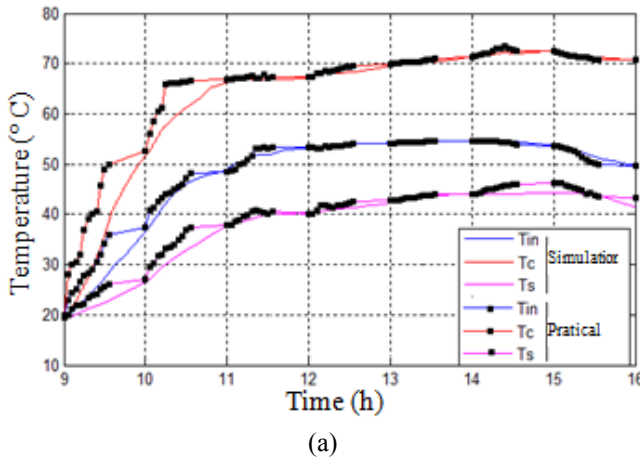


Fig. 18. Simulation and experimental results during two different days: Temperature variation, (a) day1, (b) day2.

5.4 Hybridation of solar PV/thermal system:

After these different tests devoted only to the solar thermal system, a centrifugal pump was added to pump water from the photovoltaic panels and transfer this water to the solar thermal collector. A battery was added for cloudy days in Figure 19. Different tests were performed. It is chosen a day with medium solar irradiation and another one with high irradiation. The solar water heater was filled via photovoltaic pumping water, then we carried out cycles of hot water withdrawal with simultaneous pumping with an interval of one hour. The obtained results are shown in Figure 20.

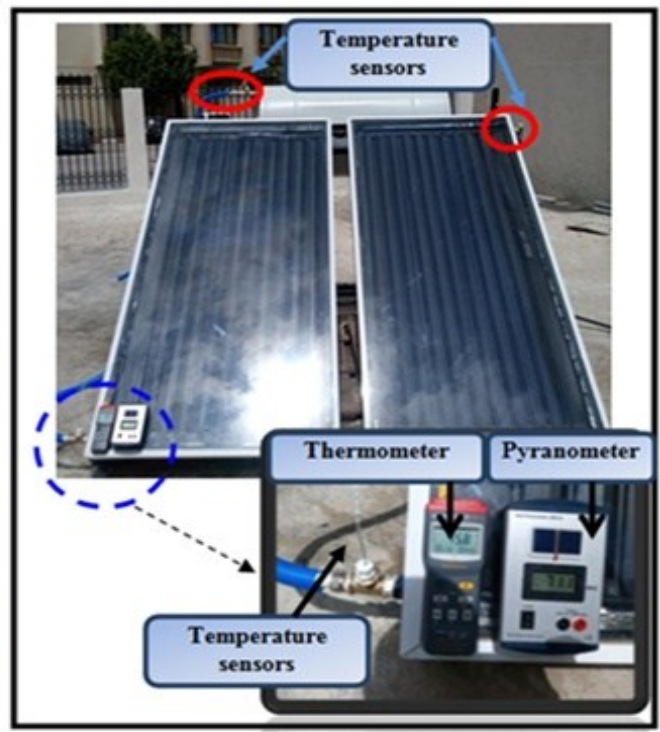
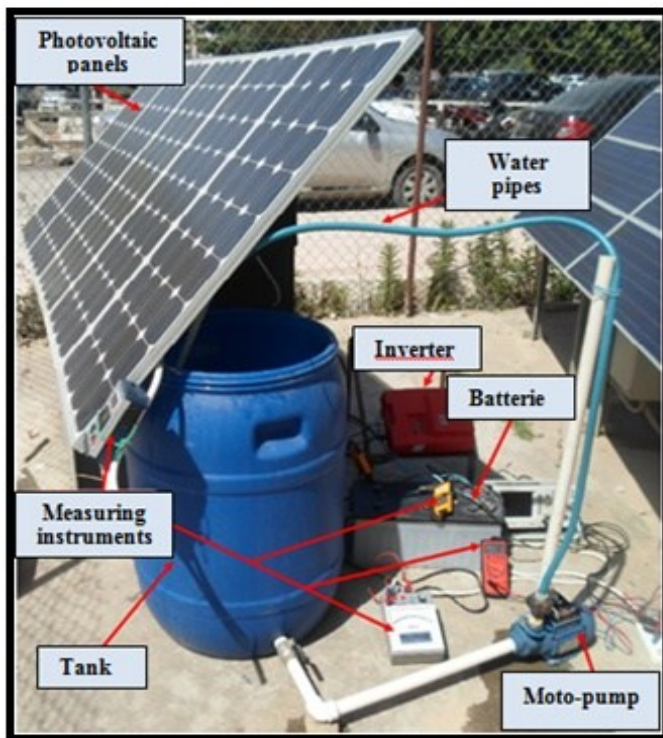


Fig. 19. Installed solar; (a) PV, (b) thermal system.

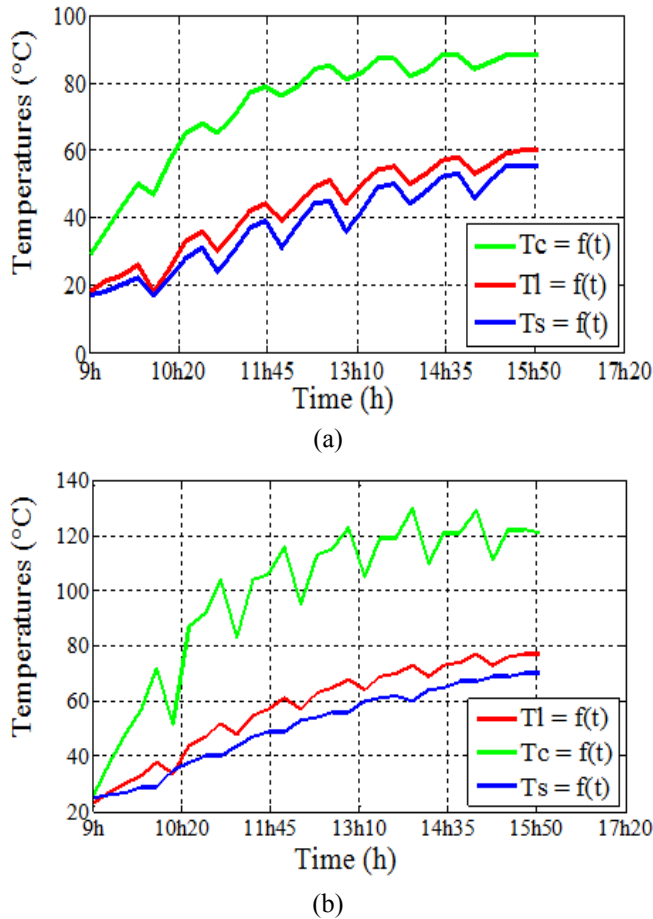


Fig. 20. Temperatures after pumping and pump-out of the sensor (T_i , T_c) and the tank output, (a) day one, (b) day two.

It can be seen that all temperatures decrease considerably just after each pump-down before returning to their normal values. It is shown a sudden increase in temperature due to the pressure from the pumped water. It is also noticed the effect of pumping-drawing by a sudden increase in temperature.

6. CONCLUSION

In this paper, the feasibility study of the solar photovoltaic/thermal system is presented. An application has been made in the laboratory in the city of Bejaia, Algeria, where solar energy is very exploitable due to its geographical location. Different tests have been made under different day profiles. The calculation of the experimental effectiveness of the heat exchanger and the daily efficiency has been made to show the influence of solar irradiance. The obtained findings seem good but can be improved. The calculation of the experimental effectiveness of the heat exchanger during two different days varies in our case from 0.5747 to 0.5815 and can be improved in the future. The results presented show a good agreement between the simulation and experimental results.

Nomenclature

A_c	Collector surface
c	Specific heat capacity of the fluid,
F_l	Volumetric flow rate of the load,

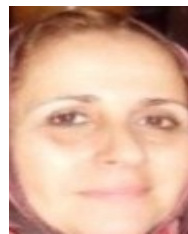
F_c	Volumetric flow rate of the collector,
I_{ph}	Light-generated current,
I_d	Diode current,
I_{Rsh}	Shunt-leakage current,
m	Fluid mass,
$N_{pv-serial}$	Serial number of PV panels,
N_{pv}	Total number of panels,
$N_{pv-para}$	Serial number of PV panels,
$Q_{uanergy}$	Energy recovered by the collector,
Q_{losses}	Energy lost by the storage tank,
R_{sh}	Shunt resistance,
T_a	Ambient temperature,
T_{abs}	Temperature of the absorber plate,
T_c	Temperature collector,
T_d	Temperature of the supplied water,
T_{in}	Fluid temperature,
T_s	Temperature of the extracted water,
U_{oc}	Open circuit voltage,
V_{st}	Volume of the storage tank,
U_L	Coefficient of overall heat loss,
τ	Transmittance of the collector cover,
α	The absorbance of the manifold, plate,
η_0	Optical efficiency,
η_{daily}	Daily efficiency,
\mathcal{E}	Effectiveness heat exchanger

References

- [1] D. Rekioua, E. Matagne, "Optimization of photovoltaic power systems: Modelization, Simulation, and Control," 2012 Series: Green Energy and Technology. Ed Springer, (2012).
- [2] E. Cuce, E. K. Oztekin, P. M. Cuce, "Hybrid photovoltaic/thermal (HPV/T) systems: From theory to applications," *Energy Research Journal*, 9, pp. 1–71, (2018)
- [3] H. A. Zondag, "Flat-plate PV-Thermal collectors and systems: A review," *Renewable Sustainable Energy Rev.*, Vol. 12, pp. 891-959, (2008).
- [4] Z. Naghibi, S. Ekhtiari, R. Carriveau, David S-K. Ting, "Hybrid solar thermal/photovoltaic-battery energy storage system in a commercial greenhouse: Performance and economic analysis", *Energy Storage*, 3(1), e215, (2021).
- [5] A. K. Dash, S. Gairola, S. Agrawal, S. Shukla, "A novel investigation and comparative study on building integrated photovoltaic thermal (BIPVT) system," *International Journal of Mathematical, Engineering and Management Sciences*, 4(2), pp. 460-470, (2019).
- [6] P. G. Charalambous, G. G. Maidment, S. A. Kalogirou, K. Yiakoumetti, "Photovoltaic thermal (PV/T) collectors: A review," *Applied Thermal Engineering*, 27(2-3), pp. 275-286, (2007).
- [7] S. A. Husain, M. Othman, N.N.W. Khalili, "A Review on the Important Key Properties of Mathematical Models Describing Photovoltaic/Thermal (PV/T) Solar Collectors System", *Studies in Systems, Decision, and Control*, Vol. 383, pp. 149–156, (2022).
- [8] D. Jain and G. N. Tiwari, "Modeling and optimal design of ground air collector for heating in controlled environment

- greenhouse", *Energy Convers Management*, 44(8), pp. 1357-72, (2003).
- [9] A. Achour, D. Rekioua, A. Mohammedi, Z. Mokrani, T. Rekioua, S. Bacha, "Application of direct torque control to a photovoltaic pumping system with sliding-mode control optimization," *Electric Power Components and Systems*, 44(2), pp. 172-184, (2016).
- [10] V. Deokar, R. S. Bindu, T. Deokar, "Simulation modeling and experimental validation of solar photovoltaic PMBLDC motor water pumping system," *Journal of Thermal Engineering*, 7(6), pp. 1392-1405, (2021).
- [11] T. Rekioua, D. Rekioua, "Direct torque control strategy of permanent magnet synchronous machines," in *Proc. of the 2003 IEEE Bologna Power Tech Conference Proceedings*, 2, art. no. 1304660, pp. 861-866, (2003).
- [12] S. Selimli, H. Dumrul, S. Yilmaz, O. Akman, "Experimental and numerical analysis of energy and exergy performance of photovoltaic thermal water collectors," *Solar Energy*, vol. 228, pp. 1-11, (2021).
- [13] J. I. Herraiz, J. Fernández-Ramos, R. Hogan Almeida, E. M Baguena, M.Castillo-Cagigal, L. Narvarte, "On the tuning and performance of Stand-Alone Large-Power PV irrigation systems," *Energy Conversion and Management:X*, Vol. 13, pp. 100175, (2022).
- [14] E. Ozbas, S. Selimli, M. Ozkaymak, A. S. S. Frej, "Evaluation of internal structure modifications effect of two-phase closed thermosyphon on performance: An experimental study," *Solar Energy*, Vol. 224, pp. 1326-1332, (2021).
- [15] H. Dumrul, S. Yilmaz, M. Kaya, İ. Ceylan, "Energy Analysis of Concentrated Photovoltaic/Thermal Panels with Nanofluids," *International Journal of Thermodynamics*, 24(3), pp. 227-236, (2021).
- [16] D. Rekioua, T. Rekioua, Y. Soufi, "Control of a grid-connected photovoltaic system", in *Proc. of the 2015 International Conference on Renewable Energy Research and Applications, ICRERA 2015*, art. no. 7418634, pp. 1382-1387, (2015)
- [17] D. Rekioua, S. Bensmail, N. Bettar, "Development of hybrid photovoltaic-fuel cell system for a stand-alone application," *International Journal of Hydrogen Energy*, 39(3), pp. 1604-1611, (2014).
- [18] D. Rekioua, "Power Management and Supervision of Hybrid Renewable Energy Systems", Ed.Springer, (2020).
- [19] M. Chikhi, R. Sellami, and N. Kasbadji Merzouk, "Thermal properties study of a solar water heater tank with a mantle exchanger," *International journal of energy optimization and engineering*, 3(1), pp. 92-100, (2016).
- [20] T. Baki, M. Tebbal, H. Berrebah, "Following the balloon temperature of a solar heater installed in Oran, Algeria," *Turkish Journal of Electromechanics & Energy*, 6(2), pp.73-79, (2021).
- [21] S. O. Amrouche, D. Rekioua, T. Rekioua, "Overview of energy storage in renewable energy systems," in *Proc. of the 2015 IEEE International Renewable and Sustainable Energy Conference, IRSEC 2015*, art. no. 7454988, (2016).
- [22] S. Lalouni, D. Rekioua, "Optimal control of a grid-connected photovoltaic system with constant switching frequency," *Energy Procedia*, Vol. 36, pp.189-199, (2013).
- [23] A. Mohammedi, D. Rekioua, T. Rekioua, S. Bacha, "Valve Regulated Lead Acid battery behavior in a renewable energy system under an ideal Mediterranean climate," *International Journal of Hydrogen Energy*, 41(45), pp. 20928-20938, (2016).
- [24] U. Sekmen, M. Yılmaz, Ö. Özdemir, A. İnce, "Effect of collection tank level on energy consumption of lifting pumps in drinking water distribution systems," *Turkish Journal of Electromechanics & Energy*, 6(1), pp.3-11, (2021).
- [25] T. Luna, J. Ribau, D. Figueiredo, R. Alves, "Improving energy efficiency in water supply systems with pump scheduling optimization", *Journal of Cleaner Production*, Vol. 213, pp. 342-356, (2019).
- [26] A. Bolognesia, C. Bragallia, C. Lenzi, S. Artina, "Energy efficiency optimization in water distribution systems," *Procedia Engineering*, Vol. 70, pp. 181-190, (2014).
- [27] H. M. Ramos, F. Vieira, D. I. C. Covas, "Energy efficiency in a water supply system: energy consumption and CO₂ emission," *Water Science and Engineering*, 3(3), pp. 331-340, (2010).

Biographies



Djamila Rekioua is a professor at the University of Bejaïa. She obtained her Ph.D. in Electrical Engineering in 2002. She is specialized in the control of electrical machines and renewable energies and has defended several Master and Ph.D. theses. She has received several awards for her research work. Her main work focuses on wind, photovoltaic, fuel cell, storage, and multi-source systems. She is the author of several international publications and scientific papers.

E-mail: djamila.ziani@univ-bejaia.dz



Saloua Belaid received her Master's diploma from the University of Bejaia in Algeria. She is a Ph.D. candidate in electrical engineering at the Electrical Engineering Department-University of Bejaia (Algeria) since 2019. Her research activities have been devoted to several topics: photovoltaic and wind systems, modeling, batteries, optimization,

hybrid systems control in AC machines.

E-mail: saloua.belaid@univ-bejaia.dz



Toufik Rekioua received his Engineer from the National Polytechnic Institute of Algiers and earned the Doctoral degree from I.N.P.L of Nancy (France) in 1991. He is a Professor at the Electrical Engineering Department-University of Bejaia (Algeria) since 1992. His research activities have been devoted to several topics: control of electrical drives, modeling, wind turbine, photovoltaic, and control in AC machines.

E-mail: toufik.rekioua@univ-bejaia.dz